Journal of Catalysis **193,** 186–198 (2000)
doi:10.1006/jcat.2000.2905, available online at http://www.idealibrary.com on IDEAL®

Preparation and Characterization of Supported Bimetallic Pt–Au and Pt–Cu Catalysts from Bimetallic Molecular Precursors

Bert D. Chandler,[1] Alexander B. Schabel, and Louis H. Pignolet

Department of Chemistry, University of Minnesota, Minneapolis, Minnesota 55455

Received August 6, 1999; revised April 25, 2000; accepted April 25, 2000

Silica-supported bimetallic Pt–Cu and Pt–Au catalysts were prepared using bimetallic molecular cluster precursors as the metal source. The molecular precursors were adsorbed onto the support from an organic solvent, dried under vacuum, calcined under flowing oxygen, and reduced with hydrogen. The resulting catalysts were characterized with CO chemisorption, diffuse reflectance Fourier transform spectroscopy (DRIFTS) of adsorbed CO, transmission electron microscopy (TEM), and energy dispersive spectroscopy (EDS). The new catalysts were also compared to traditionally prepared Pt and Pt–Cu catalysts (wetness impregnation or coimpregnation) that had been subjected to identical activation conditions. When the molecular cluster precursors were used as catalyst precursors, small and uniform bimetallic particles with high Pt dispersions were prepared. The DRIFTS spectrum of CO bound to the cluster-derived Pt–Cu catalyst was exceptionally broad and indicated a large red shift in ν(C≡O) relative to Pt. Catalytic performance was evaluated with the hexane conversion reaction. Both cluster-derived catalysts showed enhanced selectivity for light hydrocarbon production (cracking) and decreased activity for nondestructive alkane reforming and dehydrocyclization reactions. The cluster-derived catalysts had nearly identical distributions of light hydrocarbon; these distributions indicated a propensity for internal C–C bond cleavage. Despite the similarities of these fission patterns, the Pt–Au catalyst had greatly enhanced resistance to deactivation processes while the Pt–Cu had no superior deactivation performance over the traditional Pt catalyst.

Key Words: **Pt–Au catalysts; Pt–Cu catalysts; *n*-hexane conversion; supported clusters; bimetallic clusters; heterogenized catalysts.**

INTRODUCTION

Supported alloys comprised of an active group VIII metal and an "inactive" group Ib metal have been examined as catalysts for a wide variety of industrially important reactions. For example, Pd–Au alloys are widely used in the production of vinyl acetate (1), and the coimpregnation of Au with Pt has been shown to enhance emissions control catalyst properties (2). Pd–Cu alloys have also shown promise as selective hydrogenation catalysts, particularly for the selective hydrogenation of 1,3-butadiene in 1-butene, which is used in the production of polybutadiene and styrene–butadiene synthetic rubbers (3). In addition, a carbon-supported Pt–Cu catalyst is currently employed in a process for the dechlorination of chlorinated hydrocarbons to produce usable feedstocks from highly chlorinated waste streams (4). In more academic applications, supported Pt–Au catalysts played a pivotal role in the investigation of structure sensitivity in hydrocarbon reforming reactions (5–9). In addition to the utilization of amorphous supports, Pt–Cu catalysts have also been prepared and characterized within the cages of Y zeolites (10–12).

Almost ubiquitously, supported bimetallic alloy catalysts are prepared via a technique involving the adsorption, impregnation, deposition, or precipitation of monometallic precursors onto the support followed by an activation step (usually reduction) (13). A common problem that can arise from coimpregnation techniques is chromatographic separation of the precursor ions as they pass through the pore structure of the support (13). A more homogeneous alloy may be formed with high-temperature reduction or annealing; however, this risks possible excessive sintering (13). Although some techniques allow for a degree of control over metal particle sizes and distribution (14), particle composition and surface composition of metals may have wide-ranging distributions. Even when overall surface compositions are relatively homogeneous, varying degrees of clustering of one metal on the surface can produce numerous types of active sites on particles throughout the catalyst (13).

A different approach to the preparation of highly dispersed supported metal particle catalysts is to adsorb ligand-stabilized bimetallic molecular precursors (particularly inorganic and organometallic cluster compounds) onto the support and thermally remove the ligands. Past studies in this field have largely involved the use of mono- and bimetallic carbonyl clusters as precursors; several reviews on the subject are available (15–22). In most studies, molecular cluster compounds were supported on various

[1] To whom correspondence should be addressed. Current address: Department of Chemical Engineering, University of South Carolina, Swearingen Engineering Center, Columbia, SC 29208. Fax: (803) 777-8265. E-mail: chandleb@engr.sc.edu.

0021-9517/00 $35.00

oxide supports (e.g., silica, alumina, magnesia, or zeolites) and subsequently decarbonylated by heating under vacuum or inert atmosphere. Further studies have shown that in some cases the structure of the metal core remains substantially intact after ligand removal (23–25). These well-defined metal cluster catalysts have been examined with a variety of probe reactions, the results of which have important implications toward the nature of catalytic active sites (23–25).

Unfortunately, there are few bimetallic Pt–M clusters that are ligated exclusively by CO and carbonyl-ligated Pt–Cu clusters are unavailable. There are many molecular Pt–M clusters stabilized by phosphine ligands (26, 27); however, previous studies using phosphine-stabilized Pt–Au clusters as catalyst precursors indicated that that the presence of phosphine residues controls the properties of the resulting catalysts (28–32). Results showed that residual phosphorus efficiently poisons alkane reforming and C–C bond fission reactions. At the same time, the hydrogenation and dehydrogenation activity of these catalysts is relatively unaffected by the presence of phosphorus and these catalysts are being studied as selective dehydrogenation catalysts (32, 33).

Clusters stabilized by other organometallic ligand systems also hold promise as precursors to highly dispersed supported bimetallic catalysts. A recent study in our laboratory reported the preparation of Pt–Au catalysts derived from a bimetallic cluster ligated exclusively by acetylide ligands (34). Using the $Pt_2Au_4(C{\equiv}C^tBu)_8$ cluster as the catalyst precursor yielded catalysts with well-dispersed bimetallic particles. There was no evidence for large-scale metal segregation, despite the bulk immiscibility of the two metals at this ratio. Hexane conversion catalysis and characterization results indicated the particles prepared via this route may have unique compositions or morphologies that are unattainable via traditional impregnation routes. In the current study, we extend this research to include the analogous Pt–Cu cluster, $Pt_2Cu_4(C{\equiv}C^tBu)_8$. In order to make the most meaningful comparisons possible between the catalysts, additional data for the Pt and cluster-derived Pt–Au catalysts are also reported here.

METHODS

Catalyst preparation. The organometallic clusters $Pt_2Au_4(C{\equiv}C^tBu)_8$ and $Pt_2Cu_4(C{\equiv}C^tBu)_8$ were prepared from $[N(C_4H_9)_4]_2[Pt(C{\equiv}C^tBu)_4]$ and $Au(SC_4H_8)Cl$ or CuCl via literature procedures (35). Hexachloroplatinic acid, $H_2PtCl_6 \cdot 6H_2O$, was prepared from Pt metal (99.99%) according to the literature procedure (36). Cupric nitrate tetrahydrate ($Cu(NO_3)_2 \cdot 4H_2O$) was purchased from Aldrich. Davisil SiO_2 (35–60 mesh, BET surface area 360 m^2/g, average pore diameter = 150 Å) was washed with high-purity millipore distilled and deionized water to remove the fine particles and dried *in vacuo* at 120°C for 24 h prior to use. Conventional Pt, Cu, and Pt–Cu catalysts were prepared by incipient wetness impregnation and coimpregnation of the inorganic salt precursors onto the dried silica support. Solution concentrations were adjusted to give the following catalysts with % loadings: 0.15-Pt (0.15% Pt), 0.10-Cu (0.10% Cu), and 0.15-Pt + 2Cu (0.15% Pt + 0.10% Cu). The bimetallic clusters $Pt_2Cu_4(C{\equiv}C^tBu)_8$ and $Pt_2Au_4(C{\equiv}C^tBu)_8$ spontaneously adsorbed onto silica from hexanes solution. The remaining solvent was decanted and the supported clusters were dried at 60°C *in vacuo* to yield the 0.15-Pt_2Cu_4 (0.15% Pt, 0.10% Cu) and 0.15-Pt_2Au_4 (0.15% Pt, 0.30% Au) catalysts. The abbreviations indicate the atomic ratio of metals and are used only to refer to catalysts that have undergone the standard activation protocol (see below). The details of the general procedure have been previously reported for the support of phosphine-stabilized Pt and Pt–Au compounds (28, 33) and were similarly employed in this study.

Catalyst activation. Catalyst activation, chemisorption measurements, and catalytic investigations were carried out with the use of an RXM-100 catalyst characterization system purchased from Advanced Scientific Designs, Inc. Gases were all UHP grade (99.999%) and were used without further purification. In a typical experiment, 20–500 mg of the supported catalyst precursor was loaded into a U-shaped quartz microreactor (inside diameter = 11 mm), attached to the RXM-100 system, and heated in the presence of flowing gas as described below. With O_2 flowing at 10 mL/min, the temperature was ramped 10°C/min to 300°C, held for 2 h, and ramped 10°C/min back to 30°C. The sample was purged with He flowing at 100 mL/min for several minutes and the gas was switched to H_2 flowing at 20 mL/min. The temperature was then ramped 10°C/min to 200°C and held there for 1 h. This is the standard activation protocol for all experiments unless specifically stated otherwise.

Chemisorption experiments. All adsorption isotherms were measured at 21 (±2)°C over an equilibrium pressure range of 10–80 Torr. The chemisorption protocol was as follows. Following the standard activation protocol, samples were cooled 10°C/min under flowing H_2 to 135°C and evacuated for 1 h. The samples were then cooled to room temperature under high vacuum and the furnace was replaced with a water bath. The base pressure was usually below 2×10^{-7} Torr and was never higher than 5×10^{-7} Torr. A CO uptake isotherm was measured, the sample was evacuated for 35 min, and a second CO uptake isotherm was measured. All chemisorption calculations were done using Advanced Scientific Designs, Inc. software. Total CO chemisorption was determined by subtracting a physical adsorption isotherm of CO on a silica blank that had undergone identical standard activation and chemisorption protocols. The irreversibly bound CO isotherm was

determined by subtracting the second measured CO uptake isotherm from the first. The reversibly bound CO is the difference between the total CO chemisorption and the irreversible CO chemisorption. All CO uptake values are reported from the best-fit isotherm (from ASDI software) at 80 Torr.

Diffuse reflectance infrared Fourier transform spectroscopy (DRIFTS). DRIFTS studies were conducted with a Magna 750 FTIR system (Nicolet) using a DRIFTS cell (SpectraTech) equipped with an accessory that allows *in situ* treatments with different gases at temperatures up to 900°C. A liquid nitrogen-cooled MCT detector was used for data collection and OMNIC software was used for data processing. The interferograms consisted of 512 scans and the spectra were collected with a 2 cm^{-1} resolution in the absorbance format using a KBr spectrum as the background. The silica-supported precursors were activated with the standard activation protocol and cooled 10°C/min to ambient temperature on the RXM-100 system. The samples were *finely* ground with an agate mortar and pestle (important) and placed into the DRIFTS cell where they were re-reduced under a flow of H_2 at 200°C and ambient pressure. After reduction, the samples were cooled under flowing nitrogen and a spectrum was recorded at 22°C. The samples were then treated with carbon monoxide at room temperature and ambient pressure by flowing CO through the cell for 1.5 min. The cell was then flushed with nitrogen for 3 min and the spectrum of bound CO was collected. In order to best observe the peaks corresponding to bound CO, the spectrum collected before the CO treatment was subtracted from the spectrum after the CO treatment.

Transmission electron microscopy (TEM) and energy dispersive spectroscopy (EDS). Samples were prepared for TEM by crushing them with an agate mortar and pestle and dispersing about 20 mg of the powder in 2 mL of 1,2-dichloroethane by ultrasonification for 30 min. Five drops of the suspension were then dripped onto a holey carbon grid. Samples were examined by transmission electron microscopy (TEM) using a Philips CM30 TEM equipped with an LaB_6 or W filament running at 300 kV. Images were recorded on photographic film and scanned with a Microtech ScanMaker III before further analysis. Energy dispersive spectra (EDS) were recorded using an attached EDAX PV9900 energy dispersive spectrometer. Spectra were typically recorded for 200 s live time with the sample tilted 30° toward the detector.

Hexane conversion. A saturated hexane (Aldrich Chemical Co., 99+%) in hydrogen gas stream was produced with a two-stage hexane bubbler apparatus through gas dispersion frits. The second stage was submerged in an ice bath to maintain a hydrogen : hexane ratio of 16 : 1 (partial pressure of hexane = 49 Torr). The gas mixture was fed directly to the RXM-100 reaction manifold where it subsequently flowed over the catalyst bed. All catalysis was conducted at 400°C with weight hourly space velocity (WHSV = (g of hexane in feed) (g of Pt)$^{-1}$ (h)$^{-1}$) of hexane typically between 2–20 h^{-1}. Reaction products were analyzed on stream via gas chromatography using a Hewlet-Packard 5890A gas chromatograph operated with an FID detector. Product separation was achieved with a 30 ft SP-1700 coated 80/100 Chromosorb P AW packed column (Supelco) operated at 85°C and column head pressure of 100 psi. Products were identified by calibrating peak retention times with known hydrocarbons. The products were classified into five categories: *cracking* (formation of C_1–C_5 hydrocarbons), *isomerization* (MPs = 2- and 3-methylpentane), *hexenes*, *methylcyclopentane* (MCP), and *1,6 cyclization* (cyclohexane and benzene). Yields of products were measured in mass percent, and were corrected for minor impurities in the hexane feed. Control experiments with 80–100 mesh samples showed no measurable differences in catalyst activity, thus indicating that the reaction was not limited by internal mass transfer. Blank runs with plain SiO_2 showed no activity under reaction conditions.

RESULTS

A series of silica-supported platinum and Pt–M (M = Au or Cu) catalysts was prepared to study the effects of added metal and precursor type on catalyst activity, selectivity, and structure. All catalysts used in this study (Pt, Pt and Cu from inorganic salts, Pt and Cu from the $Pt_2Cu_4(C{\equiv}C^tBu)_8$ cluster, and Pt and Au from the $Pt_2Au_4(C{\equiv}C^tBu)_8$ cluster) contained 0.15 wt% Pt on silica. In order to make reasonable comparisons between the various bimetallic catalysts, the Pt : M atomic ratio was 0.5 for all bimetallic catalysts and activation protocols were identical for all catalysts. Activation conditions were chosen on the basis of temperature-programmed oxidation experiments with the supported clusters; these experiments indicated that oxidation of the acetylide ligands occurs primarily between 170 and 250°C (34).

Transmission Electron Microscopy

Detailed transmission electron microscopy (TEM) results for the 0.15-Pt and 0.15-Pt_2Au_4 catalysts have been previously reported and discussed in detail (34). Results from the microscopy studies of the 0.15-Pt catalyst were generally consistent with CO chemisorption data as particle size measurements from TEM were similar to calculations from CO uptake measurements. The 0.15-Pt_2Cu_4 catalysts were examined with TEM for this study, however, metal particles were not imaged, even at 300K× magnification. The presence of metal on the carrier was confirmed by energy dispersive spectroscopy (EDS), but even in the regions where Pt was detected there were no observable metal particles.

TABLE 1

CO Chemisorption Data

	CO uptake (μL of STP per g of catalyst)		
	Irreversible	Reversible	Total
0.15-Pt[a]	76	14	90
Cu	23	118	141
0.15-Pt + 2Cu	76	75	151
0.15-Pt_2Cu_4	151	167	313
	Adsorption normalized to CO per $PtCu_2$		
0.15-Pt[a]	0.44	0.08	0.52
Cu	0.13	0.68	0.81
0.15-Pt + 2Cu	0.44	0.43	0.87
0.15-Pt_2Cu_4	0.87	0.96	1.8

[a] Data from Ref. (34).

In the previous TEM studies (which included the 0.15-Pt and 0.15-Pt_2Au_4 catalysts) particles as small as 1–1.5 nm were observed (34). Consequently, the metal particles on the 0.15-Pt_2Cu_4 catalyst must be very small—beyond the resolution of the instrument to obtain sufficient contrast with the support to image them.

CO Chemisorption and DRIFTS of Adsorbed CO

Metal availability at room temperature was measured with CO chemisorption and DRIFT spectra of adsorbed CO were recorded (Table 1, Fig. 1). The designation of irreversibly bound CO (see Methods section) is an arbitrary one (37) as all chemisorption is ultimately reversible (38). Irreversibly bound CO has been designated as that which remains bound to the catalyst after 35 min of evacuation ($P \approx (1–4) \times 10^{-7}$ Torr). Evacuation conditions were chosen in order to estimate the availability of both Pt and Cu in the bimetallic Pt–Cu catalysts. For the 0.15-Pt catalyst, most of the CO uptake (~80%) remains after the evacuation step, whereas for the 0.1-Cu catalyst the majority of CO uptake (~80%) is only reversibly bound.

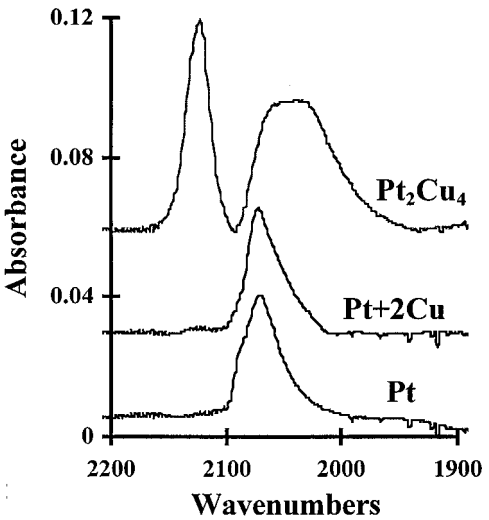

FIG. 1. DRIFTS spectra of the C≡O stretching region for carbon monoxide adsorbed to the 0.15-Pt, 0.15-Pt + 2Cu, and 0.15-Pt_2Cu_4 catalysts.

In order to more easily compare results between the bimetallic catalysts, the values in the lower portion of Table 1 have been normalized and expressed as moles of CO per $PtCu_2$. Consequently, the value reported for the 0.1-Cu catalyst is actually twice the true Cu dispersion. The catalyst prepared from the $Pt_2Cu_4(C{\equiv}C^tBu)_8$ cluster, 0.15-Pt_2Cu_4, has significantly different CO adsorption characteristics than the wetness impregnated catalysts. The total CO uptake is nearly 2 moles of CO per mole of $PtCu_2$, which is more than double the total uptake of any of the traditionally impregnated catalysts. The amount of irreversibly bound CO is also roughly double that of the 0.15-Pt or 0.15-Pt + 2Cu catalysts. The chemisorption data for this cluster derived catalyst are very similar to the data for the 0.15-Pt_2Au_4 catalyst (34).

It is possible that the catalyst pretreatment in the chemisorption protocol (evacuation at 135°C) may leave some hydrogen on the catalyst. The relatively low evacuation temperature was chosen because, with the cluster-derived catalysts, higher temperature evacuations caused inordinate losses in chemisorption. For example, evacuation of cluster-derived catalyst samples at 250°C for 2 h causes the irreversible CO uptake to be less than 10% (per total Pt). Re-reduction with H_2, followed by a lower temperature evacuation, yields the high chemisorption values. This phenomenon is completely reproducible, it is only observed with the cluster-derived catalysts, and it was never observed with the catalysts prepared from salts. In light of the TEM data, which indicate that metal particles on these catalysts are very small (*vide supra*), it is possible that high-temperature evacuation may cause some reversible morphological changes to the bimetallic particles in which the platinum becomes "buried" in the coinage metal. In order to limit the effects of this phenomenon on dispersion measurements, the evacuation treatment in the chemisorption protocol was chosen to be mild. The precision of the chemisorption measurements may be affected by residual hydrogen; however, the good agreement between CO chemisorption and TEM particle size measurements with the 0.15-Pt catalyst (34) indicates that the protocol used here does indeed provide a reasonable estimate of platinum dispersion.

DRIFTS spectra of CO bound to the freshly activated catalysts (shown in Fig. 1) also showed significant differences when the organometallic cluster was used as the metal source. CO bound to the 0.15-Pt catalyst had an adsorption band centered at roughly 2073 cm^{-1} and CO bound to the 0.1-Cu catalyst had a very weak band at roughly 2125 cm^{-1}, in good agreement with the literature

(39–43). The coimpregnated 0.15-Pt + 2Cu catalyst had a weak band at 2124 cm^{-1} assigned to CO bound to Cu. It also had a Pt–C≡O adsorption at 2075 cm^{-1} that was similar in size and shape to the corresponding band observed for the 0.15-Pt catalyst. DRIFTS spectra of the cluster-derived 0.15-Pt_2Cu_4 catalyst showed a large adsorption band at 2124 cm^{-1} resulting from CO bound to Cu. The peak assigned to the Pt–C≡O adsorption is extremely broad and is red shifted relative to the peak from the 0.15-Pt catalyst. This broad peak plateaus over energies ranging from roughly 2070 to 2020 cm^{-1}.

Hexane Conversion Catalysis

The hexane conversion reaction was chosen to evaluate the performance of the catalysts because a wide array of products can be formed (*vide infra*) and because platinum–copper and platinum–gold alloys have been previously examined for this and a variety of other hydrocarbon reactions. All experiments were carried out in a quartz micro flow reactor thermostated at 400°C with a 1 : 16 hexane : H_2 mixture at ambient pressure. Control experiments with blank silica showed no conversion of hexane under the reaction conditions. Experiments with the 0.1-Cu catalyst showed slight activity under the reaction conditions; however, the activity observed for 0.1-Cu was roughly 3–4 orders of magnitude lower than that for any of the Pt-containing catalysts. All catalyst activity measurements (Table 2) were made between 30 and 70 min on stream with total hexane conversions below 10%. Plots of conversion vs inverse space velocity (not shown) were linear for conversions below 10% and were used to determine catalyst activity.

TABLE 2

Total Activity[a] and Specific Activities[b] for Hexane Conversion Catalysis[c]

	Product class			
	Pt[d]	Pt + 2Cu	Pt_2Cu_4	Pt_2Au_4[d]
Total activity[a]	51 (4)	47 (4)	82 (5)	50 (7)
1,6 Cyclization[b]	14 (1)	8.1 (0.7)	6.5 (.1)	6.6 (0.6)
Total MCP + MPs[b]	27 (2)	27 (3)	29 (2)	24 (2)
Isomerization[b]	11 (1)	11 (1)	11 (1)	7.8 (0.3)
Cracking[b]	10 (1)	11 (1)	45 (5)	20 (1)
	Turnover frequencies (TOFs)[e] × 10^3			
Total activity[a]	106 (8)	107 (9)	94 (6)	57 (8)
1,6 Cyclization[b]	29 (3)	18 (2)	7.5 (0.2)	8 (1)
Total MCP + MPs[b]	56 (4)	62 (6)	33 (2)	27 (2)
Isomerization[b]	22 (2)	26 (3)	13 (1)	9 (1)
Cracking[b]	20 (1)	23 (2)	52 (5)	23 (2)

[a] Activity in millimoles of hexane consumed per mole of Pt per second with standard errors.

[b] Activity in millimoles of class produced per mole of Pt per second with standard errors.

[c] Catalysis at 400°C and 16 : 1 H_2 : hexane ratio at ambient pressure.

[d] Data originally reported in Ref. (34).

[e] Turnover frequencies in moles of products per mole of surface Pt per second with standard errors. CO chemisorption was used to determine platinum availability.

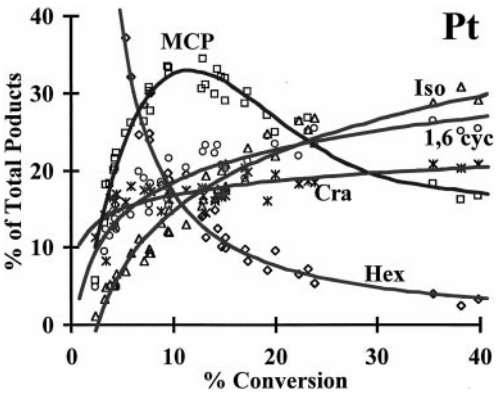

FIG. 2. Selectivity vs conversion profile for the 0.15-Pt catalyst. Hex = hexenes; Iso = isomerization (2- and 3-methylpentane); MCP = methylcyclopentane; 1,6 cyc = 1,6 cyclization (benzene and cyclohexane); Cra = light (<C6) hydrocarbons. Lines are drawn only to help see the trends.

Catalyst selectivities (reported in mass percent) were calculated from the fraction of hexane converted to a given product classification divided by the total fraction of hexane converted. All isomerization products were methylpentanes (MPs); no measurable production of dimethylbutanes was ever observed. Plots of selectivity vs conversion for the catalysts in this study are shown in Figs. 2, 3, 4, and 5. For all catalysts, hexenes are the dominant product at very low conversion (<2%) and hexene selectivity rapidly drops as conversion increases. Selectivity toward methylcyclopentane (MCP) is also high at conversions below 10%; however, MCP selectivity increases with conversion, plateaus,

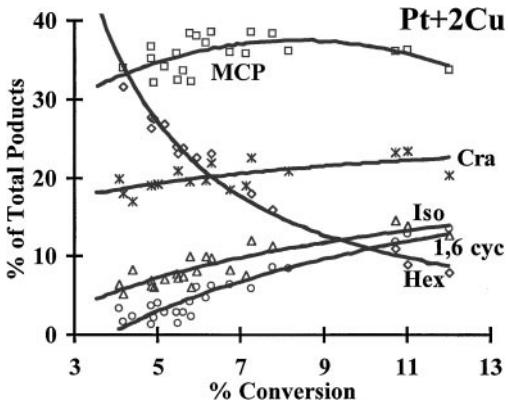

FIG. 3. Selectivity vs conversion profile for the 0.15-Pt + 2Cu catalyst. Hex = hexenes; Iso = isomerization (2- and 3-methylpentane); MCP = methylcyclopentane; 1,6 cyc = 1,6 cyclization (benzene and cyclohexane); Cra = light (<C6) hydrocarbons. Lines are drawn only to help see the trends.

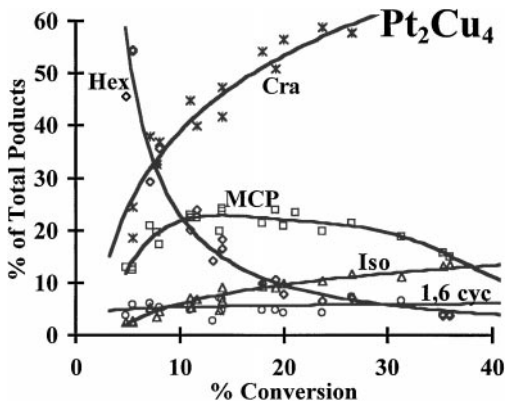

FIG. 4. Selectivity vs conversion profile for the 0.15-Pt_2Cu_4 catalyst. Hex = hexenes; Iso = isomerization (2- and 3-methylpentane); MCP = methylcyclopentane; 1,6 cyc = 1,6 cyclization (benzene and cyclohexane); Cra = light (<C6) hydrocarbons. Lines are drawn only to help see the trends.

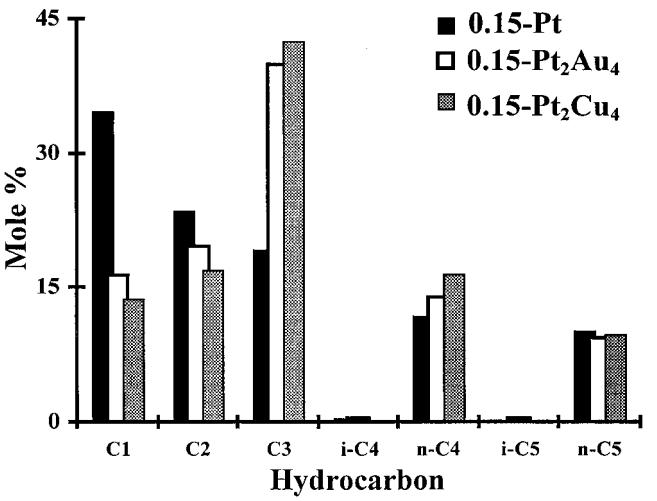

FIG. 6. Light hydrocarbon distributions at 10% conversion for the 0.15-Pt, 0.15-Pt_2Cu_4, and 0.15-Pt_2Au_4 catalysts.

and then decreases at high conversions (>20%). Simultaneously, selectivity toward cracking, isomerization, and 1,6 cyclization products increases with conversion of hexane.

The 0.15-Pt catalyst is relatively unselective for any one product class under the reaction conditions. At conversions above 15%, each of the product classes (except hexenes) ranges from about 20 to 30% of the total products. The coimpregnation of Cu with Pt in the 0.15-Pt + 2Cu catalyst slightly increases the selectivity for cracking products while decreasing selectivity for 1,6 cyclization. The cluster-derived catalysts, on the other hand, have significantly different selectivities than the wetness-impregnated catalysts. The 0.15-Pt_2Cu_4 catalyst has greatly increased selectivity for cracking products and low selectivity for MCP, 1,6 cyclization, and isomerization production. In order to make more meaningful selectivity comparisons between catalysts with different activities and dispersions, the rates of the cracking, 1,6 cyclization, 1,5 cyclization (total MCP + MPs), and isomerization were evaluated (34). The plots of production of a given product class vs inverse space velocity (not shown) were linear for conversions below 15%. The slopes of these lines give the specific activity of a catalyst for a class of reaction, i.e., the rate of production of a given product class in millimoles per mole of Pt per second. Specific activity data are compiled in Table 2, which includes corrections for CO chemisorption.

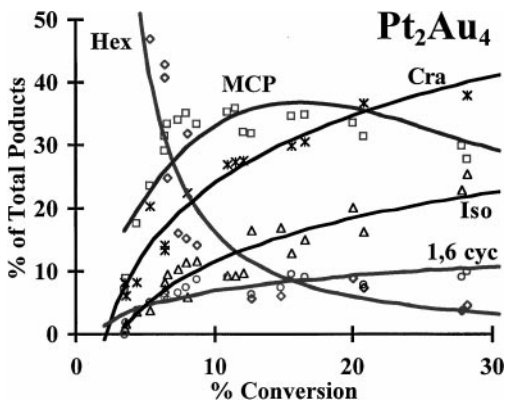

FIG. 5. Selectivity vs conversion profile for the 0.15-Pt_2Cu_4 catalyst. Hex = hexenes; Iso = isomerization (2- and 3-methylpentane); MCP = methylcyclopentane; 1,6 cyc = 1,6 cyclization (benzene and cyclohexane); Cra = light (<C6) hydrocarbons. Lines are drawn only to help see the trends.

It is apparent from Table 2 and Figs. 2 through 5 that the use of the bimetallic clusters significantly affects the activity and selectivity for C–C bond scission reactions. The distribution of C–C bond fission reaction products is similarly affected. Figure 6 shows the molar light hydrocarbon distributions for the 0.15-Pt, 0.15-Pt_2Cu_4, and 0.15-Pt_2Au_4 catalysts at 10% conversion. The distribution of light hydrocarbons did not change significantly at other conversions. The molar light hydrocarbon distribution of the 0.15-Pt catalyst indicated methane to be the dominant product, comprising slightly more than a third of the total cracking products. For the cluster-derived catalysts, propane is the predominant cracking product and the methane fraction is less than half of the 0.15-Pt catalyst's methane fraction. None of the catalysts produce significant amounts of isobutane or isopentane, which indicates that further reactions of the skeletal rearrangement products are negligible (44). Isobutane and isopentane are the expected hydrogenolysis products of 2- and 3-methylpentane (44–46) and their production can be used as a measure of the extent of secondary reactions (44).

In order to evaluate possible differences in isomerization pathways (6, 7, 47), the ratio of 2-methylpentane to 3-methylpentane was plotted versus the conversion to 1,5

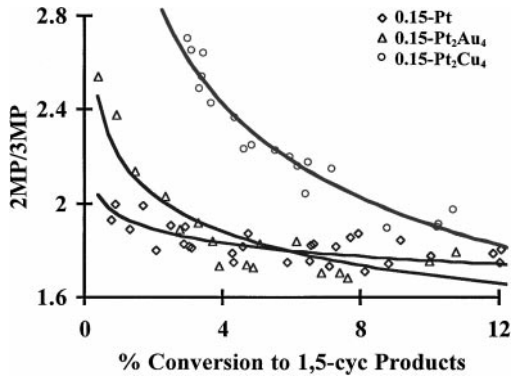

FIG. 7. Ratio of 2-methylpentane (2-MP) to 3-methylpentane (3-MP) as a function of conversion of 1,5 cyclization products for the 0.15-Pt, 0.15-Pt_2Cu_4, and 0.15-Pt_2Au_4 catalysts.

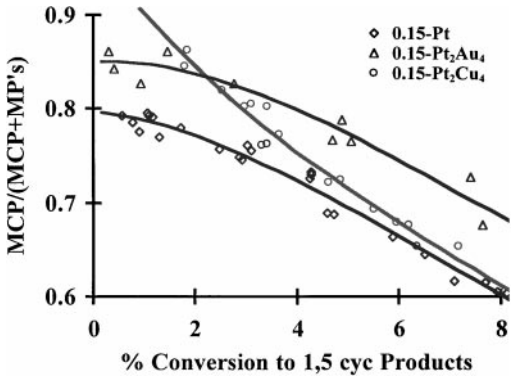

FIG. 8. MCP/(MCP + MPs) ratio vs conversion to 1,5 cyclization products for the 0.15-Pt, 0.15-Pt_2Cu_4, and 0.15-Pt_2Au_4 catalysts.

cyclization products[2] (MCP + MPs) in Fig. 7. The 0.15-Pt + 2Cu catalyst was indistinguishable from the 0.15-Pt catalyst in the plot for Fig. 7 and is omitted for clarity. Comparative evaluations of surface hydrogen were also made by plotting the ratio of MCP to 1,5 cyclization products in Fig. 8. The higher ratio observed for the cluster-derived catalysts suggests that they may be hydrogen deficient under the reaction conditions.

The catalysts were also tested for their resistance to deactivation using an initial conversion of ca. 15%. Plots for the 0.15-Pt, 0.15-Pt_2Au_4, and 0.15-Pt_2Cu_4 catalysts are shown in Fig. 9. The plot for the 0.15-Pt + 2Cu catalyst was not significantly different than those for the 0.15-Pt and 0.15-Pt_2Cu_4 catalysts and is omitted for clarity. The addition of Cu (either via coimpregnation or via the bimetallic cluster) does not appear to have any significant effect on the deactivation properties of Pt in these catalysts. The use of the $Pt_2Au_4(C{\equiv}C^tBu)_8$ cluster, however, yields a catalyst with greatly enhanced resistance to deactivation (34).

DISCUSSION

This study reports the preparation and characterization of a supported bimetallic Pt–Cu catalyst from an organometallic cluster precursor. For comparison, additional catalysis data for the 0.15-Pt and 0.15-Pt_2Au_4 catalysts (34) have been included. The activation conditions for all catalysts were chosen on the basis of temperature-programmed oxidation and reduction experiments with the organometallic clusters (60). These conditions are unlikely to be ideal for the wetness-impregnated catalysts. Genuine alloys are generally less likely to form via reduction of the oxides or oxychlorides present after calcination, rather, direct reduction of absorbed chloro precursors is preferred for alloy preparation (13, 48, 49). Data on the wetness-coimpregnated system have been included for comparison; however, the discussion will focus on the emphasis of this research, namely, the examination of the cluster-derived catalysts.

CO Chemisorption and Transmission Electron Microscopy

Carbon monoxide chemisorption data for the 0.15-Pt and 0.15-Pt_2Au_4 catalysts can be found in Ref. (34). Briefly, for the 0.15-Pt catalyst, the CO chemisorption and transmission electron microscopy (TEM) data were in good general agreement for the determination of Pt particle size. Characterization data for the 0.15-Pt_2Au_4 catalyst indicated highly dispersed bimetallic particles with high Pt dispersion. Particle size distributions for this catalyst were narrow with 90% of the observed particles being smaller than 3.5 nm.

Characterization data for the 0.15-Pt_2Cu_4 catalyst indicate that very small and highly dispersed bimetallic

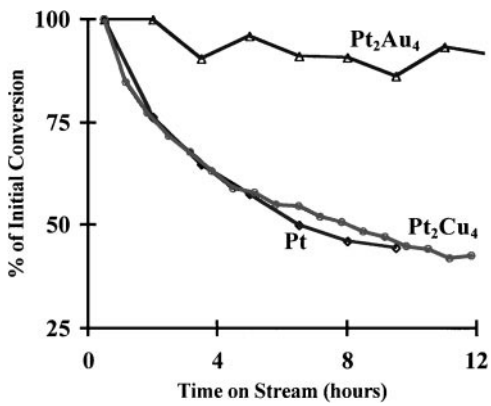

FIG. 9. Catalyst deactivation during hexane conversion catalysis for the 0.15-Pt, 0.15-Pt_2Cu_4, and 0.15-Pt_2Au_4 catalysts. Catalyst masses were adjusted so that initial conversion was ≈15% conversion of hexane.

[2] The conversion to 1,5 cyclization products (methylcyclopentane and methylpentanes) was used as the abscissa (rather than total % conversion) to ensure that only the activity for this class of reaction was being examined. When the same ratio is plotted against total % conversion, the high cracking activity of the 0.15-Pt_2Cu_4 catalyst skews the plot for this catalyst and gives a misleading representation of the data.

particles are present on the support. In order to more easily compare chemisorption data, the data in Table 1 have been normalized to moles CO per mole of $PtCu_2$ (the atomic ratio for the bimetallic catalysts). The large total CO uptakes found for the 0.15-Pt_2Cu_4 catalyst indicate excellent metal dispersions after the standard activation protocol. Using the irreversible CO uptake as an estimate of Pt availability, the chemisorption data suggest that nearly all of the Pt deposited from the clusters is available for binding of CO. In addition, the large reversible uptake of CO by this catalyst indicates Cu is also highly dispersed when the cluster is used as the catalyst precursor. These results are consistent with results for the analogous Pt–Au cluster-derived catalysts, in which high total CO uptakes were measured (>1 CO per Pt) and a similar value for irreversibly bound CO was found (34).

Attempts were made to directly evaluate metal particle size for the 0.15-Pt_2Cu_4 catalysts with TEM. At 300K× magnification, metal particles were too small to image, even on the thinnest sections of the support. Energy dispersive spectroscopy confirmed the presence of both metals in regions where particles could not be imaged. Microscopy experiments were performed on fresh samples as well as samples that had been used for other experiments (CO chemisorption, DRIFTS, catalysis). In the previous study using analogous 0.15-Pt_2Au_4 catalysts (34), particles as small as 1.5 nm were consistently imaged, which suggests that the vast majority of the metal particles on the 0.15-Pt_2Cu_4 catalyst are smaller than this value.

DRIFTS of Adsorbed CO

Diffuse reflectance infrared Fourier transform spectroscopy (DRIFTS) spectra for the Pt containing catalysts are shown in Fig. 1. The DRIFTS spectra of CO bound to the catalyst surfaces are in good agreement with other reports of Pt/silica catalysts (39–41). The value of ν(C≡O) observed for the 0.15-Pt catalyst (2073 cm^{-1}) is consistent with CO linearly adsorbed on Pt (50). Bridging carbonyls were not detected for any of the catalysts in this study, the absence of which has been previously reported for Pt/silica catalysts (39, 40). The absorbed C≡O stretching frequency for the 0.15-Pt + 2Cu catalyst (2075 cm^{-1}) is not significantly different and is also consistent with CO linearly adsorbed on Pt.

There are significant differences between the DRIFTS spectra recorded for the cluster-derived catalyst and the traditionally prepared catalysts. The large adsorption band at 2124 cm^{-1} is consistent with the large total and reversible CO uptakes measured in chemisorption experiments; the majority of the reversible chemisorption is due to CO weakly adsorbed on Cu (42, 43, 51). Although this C≡O stretch is relatively high in energy for CO bound to Cu^0 (51), it is entirely consistent with IR spectra of CO bound to reduced copper in supported Pt–Cu alloys (42, 43). The broad band ranging from roughly 2070 to 2020 cm^{-1} is consistent with previous reports of CO bound to Pt in supported Pt–Cu alloys (42, 43). Interpretation of this broad peak is difficult in light of the chemisorption and TEM results, which indicate the presence of very small bimetallic particles. One possibility is that two overlapping peaks are present, one due to CO linearly bound to Pt and a lower energy stretch arising from a bridging or semibridging mode between Pt and Cu. Previous studies with supported Pt–Cu alloys have reported similar broadening and shifts in the Pt–CO peak with adsorption on Cu sites (42, 43). Further spectroscopic characterization of these catalysts, including carbon monoxide coverage studies (52), supports this possibility.

It is not appropriate to comment on possible electronic or geometric effects of Cu on Pt based on the DRIFTS data. However, previous studies with a wide range of supported Pt–Cu alloys did not observe measurable electronic effects (43). Carbon monoxide coverage studies with the 0.15-Pt_2Cu_4 and 0.15-Pt_2Au_4 catalysts (52) also indicate that traditional alloy electronic effects are not important for the cluster-derived catalysts. For the cluster-derived catalysts, particle size effects are also expected to be important and could have significant influences on the DRIFTS spectrum of this catalyst (37). Regardless of the individual causes of the 0.15-Pt_2Cu_4 catalyst's spectroscopic characteristics, it is clear that the catalyst obtained using the bimetallic cluster as the metal source is distinctly different from the catalyst prepared via traditional coimpregnation.

Hexane Conversion Catalysis

Light hydrocarbon production. Selectivity vs conversion profiles for the catalysts are found in Figs. 2, 3, 4, and 5. The initial production of olefins followed by a rapid decrease in hexene selectivity is consistent with a rapid equilibrium in which olefin production is under thermodynamic control (53). The measured olefin concentrations are consistent with this conclusion and with calculations based on the reaction conditions (400°C, H_2 : hexane = 16) (33). It is apparent that the cluster-derived catalysts favor production of light hydrocarbons over skeletal rearrangements. The turnover frequency (TOF) data in Table 2 indicate that the increased selectivity for light hydrocarbon production is due to both the enhancement of C–C bond fission reactions and to slower rates of MCP, methylpentane, and benzene production (relative to the traditional Pt catalyst).

Light hydrocarbon production over the 0.15-Pt_2Cu_4 catalyst is more than double that of any other catalysts in this study. The increase in activity for C–C bond fission upon the alloying of Cu with Pt has been well documented (54–58). One study in particular attempted to establish the role of Cu in hydrogenolysis reactions for several Cu-containing alloys (59). The authors suggested that Cu atoms do indeed play a role in increasing rates of hydrogenolysis (in contrast

to Au and Ag which decrease hydrogenolysis rates), possibly by participating in the binding of hydrocarbon intermediates via a "mixed ensemble". The broad Pt–CO peak in the DRIFTS spectrum of CO adsorbed on the 0.15-Pt_2Cu_4 catalyst could possibly be evidence for such a binding motif (60). Previous investigations have also suggested that "the individuality of the [active] transition metal atoms is possibly preserved in the alloys" (59). Results with the 0.15-Pt_2Cu_4 and 0.15-Pt_2Au_4 catalysts are consistent with this observation, as there are no significant differences in the light hydrocarbon distributions of these two catalysts (*vide infra*).

For the 0.15-Pt_2Au_4 catalyst, the total production of light hydrocarbons is not significantly faster than over 0.15-Pt; however, hydrogenolysis reactions are indeed slower. The term "hydrogenolysis" is often used in several slightly different ways. We specifically refer to *hydrogenolysis* reactions as terminal C–C bond fission reactions and use the term *nonhydrogenolytic* cracking to describe internal C–C bond cleavage. This is an important distinction as the two processes may involve different mechanisms with very different binding motifs and surface intermediates. Because nonhydrogenolytic cracking involves internal bond cleavage, the hydrocarbon must be bound in a fashion that is more parallel to the catalyst surface. Conversely, we interpret hydrogenolysis reactions to involve an "end-on" binding motif for the hydrocarbon. Notably, both processes can produce methane, but only nonhydrogenolytic cracking can produce two fragments that are both C2 or greater. Using these definitions to interpret the light hydrocarbon distributions in Fig. 6, the cluster-derived catalysts clearly have lower hydrogenolysis activities than the traditionally prepared catalysts, even though the overall cracking activity (total light hydrocarbon production) may be greater.

This is an important distinction. First, hydrogenolysis reactions are known to be very structure sensitive (6, 8, 13, 53). The distribution data from 0.15-Pt (large methane fraction) suggest that hydrogenolytic cracking is the dominant C–C bond fission mechanism. Further, the asymmetry of the distribution indicates that individual substrate molecules undergo successive hydrogenolytic cracking steps on the metal particles (34), i.e., a single hexane molecule may be converted to more than one methane and a C4 or smaller fragment without desorbing from the metal particle. The symmetry of the cluster-derived catalysts' light hydrocarbon distributions indicates that that hydrogenolytic cracking mechanisms have little or no influence on the overall cracking activity. Because the characterization data indicate that both catalysts have small and bimetallic particles, these results are entirely consistent with the well-known sympathetic structure sensitivity of hydrogenolysis reactions (8, 13).

This distinction is also important in light of the very low selectivity for benzene formation and the literature regarding highly dispersed platinum on alkaline supports. The discovery of high aromatization activity during using very highly dispersed platinum on nonacidic L-zeolite (61) or on amorphous magnesia (62, 63) has sparked a renaissance in research on alkane conversion over supported Pt catalysts. Further studies with several catalysts comprised of platinum on an alkaline support reveal that the correlations initially reported for Pt/KL-zeolite hold for the other supports; namely, that increased benzene selectivity correlates with (i) increased support basicity, (ii) decreased C≡O stretching frequencies of carbon monoxide adsorbed to the metal surface, and (iii) increased propensity for terminal hydrogenolysis (44). Comparisons between our results and these studies are tenuous because of the large differences in alkalinity between silica and magnesia or KL-zeolite. At the same time, results with the cluster-derived catalysts are generally consistent with the catalysis results with Pt on alkaline supports: the cluster-derived catalysts favor internal over terminal C–C bond fission and aromatization activity is suppressed.

Mechanisms of alkane reforming. We believe that the catalysis results with the cluster-derived catalysts are most appropriately understood in terms of the traditional mechanisms of alkane reforming over silica- and alumina-supported Pt catalysts. Before examining the possible reaction mechanisms at work, the thermodynamics of the reaction system should be considered. The five structural isomers of hexane are essentially thermoneutral and are significantly more stable at ambient temperatures than are cycloalkanes or benzene (47). Methylcyclopentane (MCP) formation is favorable at temperatures above 323°C and benzene formation is even more so. Cyclohexane is thermodynamically unstable above 223°C due to the stability of benzene (47) and only a small concentration of olefins (at equilibrium) can coexist with paraffins in excess hydrogen at temperatures below about 500°C (6). Despite the loss of dihydrogen, cyclization reactions are entropically unfavorable. From *n*-hexane, C5 cyclization costs roughly 16 entropy units (eu); cyclohexane and benzene formation correspond to a loss of about 25 and 38–45 eu, respectively (47). These entropy losses are comparable to calculated entropies of adsorption (64), which suggests that one of the major roles of the catalyst is to adsorb the substrate in a geometry favorable for cyclization (47).

The mechanisms of metal-catalyzed hydrocarbon reactions have been inferred from a wide variety of reaction studies, which have proven to be particularly useful in providing insight to the substrate binding motifs over various metals (6, 7, 13, 37, 47, 53, 64–66). These proposed mechanisms were largely developed over supported metal and alloy catalysts using nonacidic and nonalkaline supports, i.e., silicas and aluminas rather than alkaline zeolites or magnesia. Particularly for isomerization reactions, individual

mechanisms can differ from one hydrocarbon to another and are greatly affected by particle size, ensemble sizes, crystallographic orientation of the exposed metal surface, and acidity/alkalinity of the support. Surface hydrogen effects also play an important role in determining the relative rates of competing reactions (hence the amounts of the various products) without directly altering the mechanisms at work (47, 53).

Because benzene is a deep thermodynamic sink for the C6 system, it has been inferred that direct ring enlargement reactions to form cyclohexane from MCP are not catalyzed by metals (47, 53). It is then assumed that there are two general types of surface intermediates available. One yields methylcyclopentane and isomers while the other yields benzene; interconversion between the two types of intermediates must be strongly inhibited (47). The surface intermediate(s) for benzene production over metals has been proposed to be a deeply dehydrogenated (polyunsaturated) open-chain molecule such as a bound diene or triene (67). This suggests that, over metals, aromatization reactions are more closely related to dehydrogenation reactions than they are to cyclizations.

The reaction network displayed in Fig. 10 indicates that *n*-hexane, methylpentances, and methylcyclopentane are all related through a single interconversion step. Two general mechanisms have been proposed for the isomerization of hydrocarbons by metal catalysts. The "bond shift" mechanism is the more general mechanism in that it has been shown to be viable on a wide variety of metals (7, 8, 13, 47). The proposed surface intermediates are essentially built around a cyclopropane-like structure. An important mechanistic consideration that arises from the bond shift mechanism is that all of the possible C_6H_{14} isomers can be produced from hexane. Most notably, through two successive cyclization steps, 1,1- and 1,2-dimethyl butane can be produced.

For Pt, Pd, Ir, and Rh, an additional isomerization pathway is available. With hexane and larger hydrocarbons, isomerization can occur by cyclization of the alkane to a substituted cyclopentane followed by ring opening at a different bond (7, 8, 13, 47). C5 cyclizations (the "cyclic" mechanism) require additional hydrogen and are accelerated by increased hydrogen pressures (47), despite the net production of hydrogen by the reaction. Further, C5 cyclic isomerization can occur over large ensembles or at sites where the substrate binds to a single metal atom (47, 68). For some of the proposed intermediates, a "dual site" mechanism has been proposed in which the intermediate lies parallel to the metal surface (68).

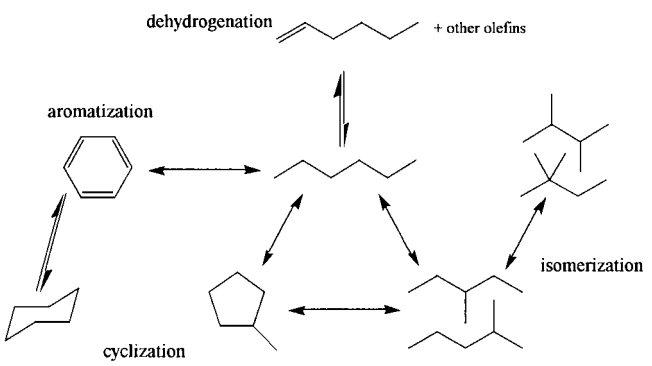

FIG. 10. Reaction network for platinum-catalyzed skeletal rearrangements of C6 hydrocarbons.

Alkane reforming over cluster-derived catalysts. Although the relative contributions of the two mechanisms cannot be definitively evaluated without proper labeling studies (65, 69), the results with the catalysts in this study are generally consistent with the cyclic mechanism. The maximum in MCP selectivity (with conversion) is strong evidence that MCP is the primary skeletal rearrangement product and that the methylpentanes are formed subsequent to the production of MCP. The dominance of the cyclic mechanism is also supported by the lack of production of dimethylbutanes. If the bond shift mechanism significantly contributed to the production of isomerization products, considerable amounts of dimethylbutanes should be observed at higher conversions. Because the reaction conditions include hydrogen pressures 16 times greater than that of hexane, the dominance of the cyclic mechanism is not surprising as reactions via this mechanism are accelerated by higher hydrogen pressures (47). Further, the "MCP surface intermediate" is known to be present in reactions over Pt–Au and Pt–Cu alloys (8). The small Pt ensembles throughout these alloys have been suggested to better accomodate the five-member cyclic intermediate (8).

Measurement of the rate of MCP production in the same manner as was used for the other product classes was not possible because plots of MCP fraction vs inverse space velocity were not linear. This is consistent with the selectivity vs conversion profiles and the dominance of the cyclic mechanism. Therefore, the sum of MCP + MPs was used to estimate the rate of 1,5 cyclization and is included as one of the specific activities in Table 2. Total conversion to 1,5 cyclization products was also used in examining the 2-methylpentane to 3-methylpentane ratio as described below. In doing this, several assumptions were made based this mechanism: (i) the bond shift mechanism does not appreciably account for the production of 2-MP and 3-MP (6); (ii) ring enlargement, i.e., conversion of MCP to cyclohexane or benzene, is not a viable reaction pathway (70); and (iii) further reaction of MCP or methylpentanes (i.e., cracking) does not appreciably occur. The last assumption is supported by the lack of significant isopentane or isobutane production (44–46).

The ratio of 2-MP to 3-MP selectivity (Fig. 7) indicates that the isomerization pathway differs slightly on the

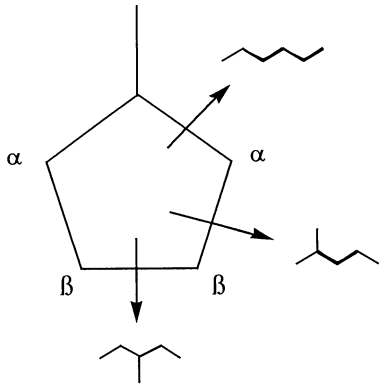

FIG. 11. Relationships between C_6H_{14} isomers and the C5 cyclic intermediate.

various catalysts. Figure 11 shows how cleaving the different C–C bonds of an adsorbed C5 cyclic intermediate (MCP) can lead to the production of the available hexane isomers. Cleavage between the tertiary carbon and an α carbon yields hexane (no observed reaction), cleavage between an α and a β carbon yields 2-MP, and cleavage between the two β carbons yields 3-MP. For 0.15-Pt, the 2-MP/3-MP ratio is always close to the statistical value of 2, as is expected for "nonselective" isomerization by Pt particles (13). Essentially, once the five-member ring is formed on the Pt particle, it has a roughly equal chance of being cleaved at any of the bonds. The cluster-derived catalysts, particularly 0.15-Pt_2Cu_4, show greater proportions of 2-MP at low conversions; i.e., the α-β carbon bonds are preferentially broken. The 1,5 cyclization necessarily occurs between atoms that become the tertiary and α carbons of the C5 cyclic intermediate. Over the cluster-derived catalysts, cleavage of the β–β carbon bond (the bond farthest from where the cyclization occurs) is much slower than cleavage of the closer α–β carbon bond. At higher conversions (longer residence times), readsorption of the methylpentanes eventually "equilibrates" the isomers, resulting in 2-MP/3-MP ratios near 2. Considering indications that the surface intermediate may be a flatly adsorbed ring (47), we conclude that the cluster-derived catalysts do not have as many nearby Pt atoms available to rapidly cleave the β–β carbon bond. This interpretation is consistent with the preparation of very small and bimetallic particles and is supported by the TEM data for both catalysts. For the 0.15-Pt_2Au_4 catalyst, particles are significantly larger (34) than for the analogous Pt–Cu catalyst and greater numbers of multiple platinum atom ensembles are expected. Consequently, the 2-MP/3MP ratio approaches 2 much more quickly over the Pt–Au catalyst than it does over the Pt–Cu catalyst.

Because 1,5 cyclization to MCP has been suggested to be hydrogen controlled (53), the slower rate of 1,5 cyclization reactions over the cluster-derived catalysts suggests the possibility that there are significant differences in available surface hydrogen. The amount of available surface hydrogen under the reaction conditions is affected by several factors such as binding affinities and surface coverage of various reaction intermediates, coke formation, and spillover onto the support. Unfortunately, it is not feasible to readily and directly quantify available hydrogen during the reaction. Although not an absolute measure, relative amounts of surface hydrogen can be qualitatively compared by plotting the ratio of methylcyclopentane to 1,5 cyclization products as a function of conversion (53) (to 1,5 cyclization products, *vide supra*). The low conversion portion of the plots in Fig. 8 suggests that the cluster-derived catalysts may have less surface hydrogen under the reaction conditions than the 0.15-Pt catalyst. This conclusion is also supported by hydrogen chemisorption experiments, which indicate lower hydrogen uptake capacities at ambient temperatures (71). The reduced levels of surface hydrogen may be an important factor in slowing 1,5 cyclization reactions over the cluster-derived catalysts.

Another consideration for differences between the cluster-derived catalysts and the traditionally prepared catalysts is that different forms of carbon are deposited on the smaller bimetallic particles. The types and quantities of surface carbon are well known to be important in determining activities and selectivities of catalysts (53). Because particle size distributions did not change significantly after hexane conversion catalysis (34), the primary mode of deactivation is presumed to be coking of the catalyst. Consequently, the possibility that carbon fouling of different sites on the various catalysts cannot be excluded.

Resistance to deactivation. Plots of overnight catalysis runs for 0.15-Pt and the cluster-derived catalysts appear in Fig. 9. In our previous manuscript (34), we hypothesized that the increased resistance to deactivation processes by cluster-derived Pt–Au catalysts might be a result of the decreased hydrogenolysis activity (34). The data for the 0.15-Pt_2Cu_4 catalyst suggest otherwise. The light hydrocarbon distributions from the two cluster-derived catalysts are nearly indistinguishable; however, it is clear from the deactivation plots that the addition of copper to platinum via the bimetallic precursor does not impart significant resistance to deactivation. The resistance to deactivation appears to be an intrinsic property of Au or of the Pt–Au particles. One possibility is that Au imparts different particle morphologies or ensemble geometries that are resistant to catalyst poisoning, although comments on any similarities or differences in particle morphologies between the two cluster-derived catalysts are little more than speculation. The suggested participation of Cu in C–C bond fission reactions (59) might also work against any resistance to deactivation that the cluster-derived particle morphology imparts.

SUMMARY

Ligand-stabilized organometallic cluster precursors have been used to prepare highly dispersed bimetallic catalysts

that are active in alkane conversion reactions. Both the 0.15-Pt_2Au_4 and 0.15-Pt_2Cu_4 catalysts have enhanced selectivity for the production of lighter hydrocarbons; the 0.15-Pt_2Cu_4 catalysts in particular have significantly increased rates of C–C bond fission. The DRIFTS spectrum of carbon monoxide adsorbed to this catalyst contains a very broad and asymmetric peak associated with CO bound to Pt. One possible interpretation of this peak is that it results from overlapping linear Pt–C≡O stretches and lower energy C≡O stretches from bridging or semibridging modes between Pt and Cu.

Differences in activity for skeletal rearrangements can be explained in terms of the cyclic mechanism of isomerization and support the characterization data that very small and bimetallic particles are prepared using the cluster precursors. Both of the cluster-derived catalysts have very similar light hydrocarbon distribution patterns and favor internal rather than terminal bond scission. At the same time, the 0.15-Pt_2Au_4 catalyst has significantly enhanced resistance to deactivation processes relative to the 0.15-Pt_2Cu_4 catalyst and a traditionally prepared Pt catalyst. Results with the 0.15-Pt_2Cu_4 catalyst indicate that this is not merely due to a lesser degree of successive terminal hydrogenolysis reactions by the 0.15-Pt_2Au_4 catalyst; rather, it may be an intrinsic property of Au that is expressed by the bimetallic particles prepared using the cluster precursor method.

ACKNOWLEDGEMENTS

We thank professors Zoltán Páal and M. Albert Vannice for their helpful discussions regarding the new catalysts. This research was funded by a grant from the University of Minnesota Graduate School. A.B.S. was a participant in an NSF-REU program in the Department of Chemistry at the University of Minnesota.

REFERENCES

1. Schwank, J., *Gold Bull.* **18**, 1 (1985).
2. Nakatsuji, T., European Patent 0 602 602 A1, 1993.
3. Furlong, B. K., Masters thesis, Rice University, Houston, TX, 1994.
4. Harley, D. A., Holbrook, M. T., Ito, L. N., Murchison, C. B., and Smith, D. D., U.S. Patents EP640577 and EP640574 and references cited therein, 1995.
5. Boudart, M., *Adv. Catal.* **20**, 153 (1969).
6. Gates, B. C., Katzer, J. R., and Schuit, G. C. A., "The Chemistry of Catalytic Processes." McGraw-Hill, New York, 1979.
7. Gault, F. G., *Adv. Catal.* **30**, 1 (1981).
8. Ponec, V., *Adv. Catal.* **32**, 149–214 (1983).
9. Yeates, R. C., and Somorjai, G. A., *J. Catal.* **103**, 208–212 (1987).
10. Tebassi, L., Sayare, A., Ghorbel, A., Dufaux, M., and Nacce, C., *J. Mol. Catal.* **25**, 397–408 (1984).
11. Moretti, G., and Sachtler, W. M. H., *J. Catal.* **115**, 205–216 (1989).
12. Ahn, D. H., Lee, J. S., Nomura, M., Sachtler, W. M. H., Moretti, G., Woo, S. I., and Ryoo, R., *J. Catal.* **133**, 191–201 (1992).
13. Ponec., V., and Bond, G. C., *in* "Catalysis by Metals and Alloys" (B. Delmon and J. T. Yates, Eds.), Studies in Surface Science and Catalysis, Vol. 95. Elsevier, Amsterdam, 1995.
14. Lam, Y. L., and Boudart, M., *J. Catal.* **50**, 530 (1977).
15. Anderson, J. R., and Mainwaring, D. E., *J. Catal.* **35**, 162 (1974).
16. Anderson, J. R., Elmes, P. S., Howe, R. F., and Mainwaring, D. E., *J. Catal.* **50**, 508 (1977).
17. Iwasawa, Y., and Yamada, M., *J. Chem. Soc., Chem. Commun.* 675 (1985).
18. Guczi, L., 7th National Symposium on Catalysis, (P. Rao, Ed.), pp. 613–620. Wiley, New York, 1985.
19. Guczi, L., *Stud. Surf. Sci. Catal.* **29**, 231–258 (1986).
20. Gates, B. C., Guczi, L., and Knozinger, H., *in* "Metal Clusters in Catalysis" (B. Delmon and J. T. Yates, Eds.), Studies in Surface Science and Catalysis, Vol. 29. Elsevier, Amsterdam, 1986.
21. Gonzalez, R. D., *Catal. Rev. Sci. Eng.* **36**, 145–177 (1994).
22. Ugo, R., Dossi, C., and Psaro, R., *J. Mol. Catal. A* **107**, 13 (1996).
23. Deutsch, S. E., Xiao, F. S., and Gates, B. C., *J. Catal.* **170**, 161 (1997).
24. Zhao, A., and Gates, B. C., *J. Catal.* **168**, 60 (1997).
25. Alexeev, O., Panjabi, G., and Gates, B. C., *J. Catal.* **173**, 196 (1998).
26. Pignolet, L. H., Aubart, M. A., Craighead, K. L., Gould, R. A. T., Krogstad, D. A., and Wiley, J. S., *Coord. Chem. Rev.* **143**, 219 (1995).
27. Pignolet, L. H., *in* "Catalysis by Di- and Polynuclear Metal Cluster Complexes" (R. D. Adams and F. A. Cotton, Eds.), pp. 95–126. VCH, New York, 1997.
28. Graf, I. V. G., Bacon, J. W., Curley, M. E., Ito, L. N., and Pignolet, L. H., *Inorg. Chem.* **35**, 689 (1996).
29. Graf, I. V. G., Ph.D. thesis, University of Minnesota, Minneapolis, MN, 1996.
30. Yuan, Y., Asakura, K., Wan, H., Tsai, K., and Iwasawa, Y., *Chem. Lett.* 129 (1996).
31. Rubinstein, L. I., Ph.D. thesis, University of Minnesota, Minneapolis, MN, 1997.
32. Chandler, B. D., Schabel, A., and Pignolet, L. H., *in* "Catalysis of Organic Reactions" (F. E. Herkes, Ed.), pp. 607–614. Dekker, New York, 1998.
33. Chandler, B. D., Rubinstein, L. I., and Pignolet, L. H., *J. Mol. Catal.* **133**, 267–282 (1998).
34. Chandler, B. D., Schabel, A. B., Blanford, C. F., and Pignolet, L. H., *J. Catal.* **187**, 367 (1999).
35. Espinet, P., Fornies, J., Martinez, F., Tomas, M., Lalinde, E., Moreno, M. T., Ruiz, A., and Welch, A. J., *J. Chem. Soc., Dalton Trans.* 791 (1990).
36. Giedt, D. C., and Nyman, C. J., *Inorg. Synth.* **8**, 239 (1966).
37. Che, M., and Bennett, C., *Adv. Catal.* **36**, 55 (1989).
38. Kip, B. J., Duivenvoorder, F. B. M., Koningsberger, D. C., and Prins, R., *J. Catal.* **105**, 26 (1987).
39. Balakrishnan, K., Sachdev, A., and Schwank, J., *J. Catal.* **121**, 441 (1990).
40. Bartok, M., Sarkany, J., and Sitkei, A., *J. Catal.* **72**, 236 (1981).
41. Haaland, J. L., *Surf. Sci.* **185**, 1 (1987).
42. Toolenaar, F. J. C. M., Reinalda, D., and Ponec, V., *J. Catal.* **64**, 110–115 (1980).
43. Toolenaar, F. J. C. M., Stoop, F., and Ponec, V., *J. Catal.* **82**, 1 (1983).
44. Menacherry, P. V., and Haller, G. L., *J. Catal.* **177**, 175 (1998).
45. Leclercq, G., Leclercq, L., and Maurel, R., *J. Catal.* **50**, 87 (1977).
46. Garin, F., Aeiyach, S., Legare, P., and Maire, G., *J. Catal.* **77**, 323 (1982).
47. Paál, Z., *Adv. Catal.* **29**, 273 (1980).
48. de Jongste, H. C., and Ponec, V., *J. Catal.* **64**, 228 (1980).
49. Bond, G. C., and Yide, X., *J. Mol. Catal.* **25**, 141 (1984).
50. Hollins, P., *Surf. Sci. Rep.* **16**, 51 (1992).
51. Dandekar, A., and Vannice, M. A., *J. Catal.* **178**, 621–639 (1998).
52. Chandler, B. D., and Pignolet, L. H., *Catal. Today*, in press.
53. Paál, Z., *in* "Hydrogen Effects in Catalysis" (Z. Paál and P. G. Menon, Eds.), p. 449. Dekker, New York, 1988.
54. de Jongste, H. C., Kuijers, F. J., and Ponec, V., *in* "Proceedings, 6th International Congress on Catalysis, London, 1976" (G. C. Bond, P. B. Wells, and F. C. Tompkins, Eds.), p. 915. The Chemical Society, London, 1977.
55. de Jongste, H. C., Ponec, V., and Gault, F. G., *J. Catal.* **63**, 395 (1980).
56. Botman, M. J. P., de Jongste, H. C., and Ponec, V., *J. Catal.* **68**, 9 (1981).

57. de Jongste, H. C., and Ponec, V., *in* "Proceedings, 7th International Congress on Catalysis, Tokyo, 1980" (T. Seiyama and K. Tanabe, Eds.), p. 186. Elsevier, Amsterdam, 1981.
58. den Hartog, A. J., Rek, P. J. M., and Ponec, V., *J. Chem. Soc., Chem. Commun.* 1470 (1988).
59. de Jongste, H. C., and Ponec, V., *J. Catal.* **63**, 389 (1980).
60. Chandler, B. D., Ph.D. thesis, University of Minnesota, Minneapolis, MN, 1999.
61. Bernard, J. R., Fifth International Congress on Zeolites, (L. V. L. Rees, Ed.), p. 686. Heyden, London, 1980.
62. Davis, R. J., and Derouane, E. G., *Nature* **349**, 313 (1991).
63. Davis, R. J., and Derouane, E. G., *J. Catal.* **132**, 269–274 (1991).
64. Kemball, C., *Adv. Catal.* **11**, 223 (1959).
65. Anderson, J. R., *Adv. Catal.* **23**, 1–90 (1973).
66. Clarke, J. K. A., and Rooney, J. J., *Adv. Catal.* **25**, 125 (1976).
67. Amir-Ebrahimi, V., and Gault, F. G., *J. Chem. Soc., Faraday Trans.* **76**, 1735 (1980).
68. Paál, Z., Dobrovolszky, M., and Tetenyi, P., *J. Catal.* **45**, 189 (1976).
69. O'Cinneide, A., and Gault, F. G., *J. Catal.* **37**, 311 (1974).
70. Paál, Z., Zhan, Z., Manninger, I., and Sachtler, W. M. H., *J. Catal.* **155**, 43 (1995).
71. Chandler, B. D., Schabel, A. S., and Pignolet, L. H., submitted for publication.